Gas Processing Journal

Vol. 8, No. 1, 2020, pp. 83-92
http://gpj.ui.ac.ir

DOI: http://dx.doi.org/10.22108/gpj.2020.119977.1069

Artificial Intelligence-based Modeling of Interfacial Tension for Carbon Dioxide Storage

Amir Hossein Hosseini [1], Hossein Ghadery-Fahliyany [2], David Anthony Wood [3*], Abouzar Choubineh [4]

[1] Petroleum Department, Semnan University, Semnan, Iran
[2] Petroleum Department, Shahid-Bahonar University, Kerman, Iran
[3] DWA Energy Limited, Lincoln, United Kingdom
[4] Petroleum Department, Petroleum University of Technology, Ahwaz, Iran

Received: 2019-11-16 Revised: 2020-01-27 Accepted: 2020-04-04

Abstract: A key variable for determining carbon dioxide (CO_2) storage capacity in sub-surface reservoirs is the interfacial tension (IFT) between formation water (brine) and injected gas. Establishing efficient and precise models for estimating CO_2 – brine IFT from measurements of independent variables is essential. This is the case because laboratory techniques for determining IFT are time-consuming, costly and require complex interpretation methods. For the datasets used in the current study, correlation coefficients between the input variables and measured IFT suggest that CO_2 density and pressure are the most influential variables, whereas brine density is the least influential. Six artificial neural network configurations are developed and evaluated to determine their relative accuracy in predicting CO_2–brine IFT. Three models involve multilayer perceptron (MLP) tuned with Levenberg-Marquardt, Bayesian regularization and scaled conjugate gradient back-propagation algorithms, respectively. Three models involve the radial basis function (RBF) trained with particle swarm optimization, differential evolution, and farmland fertility optimization algorithms, respectively. The six models all generate CO_2– brine IFT predictions with high accuracy (RMSE <0.7 mN/m). However, the RBF models consistently provide slightly higher IFT prediction accuracies (RMSE <0.54 mN/m) than the MLP models.

keywords: Interfacial Tension (IFT), CO_2 Storage, Multi-Layer Perceptron, Radial Basis Function, Neural Network Prediction, IFT Influencing Variables

1. Introduction

Storing CO_2 in depleted oil and gas reservoirs or deep saline aquifers is an attractive technology with the potential for reducing CO_2 emissions to the atmosphere, which are now established as the main cause of global warming (Abedini & Torabi, 2014). The features of porous media which are suitable for CO_2 storage are known (McGrail, Schaef, Ho, Chien, Dooley, & Davidson, 2006) to include:

1. Capacity to accept high quantities of CO_2;
2. Injectivity to absorb CO_2 at rates generated by large-scale carbon dioxide emitters;
3. Confinement (sealing) sufficient to avoid the dispersal and leakage of buoyant and portable CO_2 from the subsurface reservoirs to other below-ground formations, shallow aquifers and/or ultimately back to the Earth's surface and atmosphere.

Reservoirs at various depths can effectively store CO_2 in the subsurface and at diverse physical and chemical conditions due to the characteristics of CO_2 at the temperature and pressure states found in Earth's subsurface (Pranesh, 2018). The distinct mechanisms of entrapment are involved: initially, injected CO_2 is trapped by primary mechanisms, involving static and hydrodynamic trapping; subsequently, secondary mechanisms, including mineralization and chemical interactions between the CO_2 and the formation minerals, act to influence CO_2 containment, not necessarily to increase storage capacity (Metz, Davidson, De Coninck, Loos, & Meyer, 2005).

Storing carbon dioxide in subsurface reservoirs is vulnerable to potential problems and impacted by various uncertainties, some of which may occur during and/or after the

* Corresponding Author.
Authors' Email Address: [1] A. H. Hosseini (s.amirhosein69@yahoo.com), [2] H. Ghadery-Fahliyany (ghadery.pe@gmail.com), [3] D. Anthony Wood (dw@dwasolutions.com), [4] A. Choubineh (abouzar68choubineh@gmail.com)

ISSN (Online): 2345-4172, ISSN (Print): 2322-3251

injection stage (Damen, Faaij, & Turkenburg, 2003). The most important potential problem is CO_2 leakage. Both reservoir pressure and the buoyancy of carbon dioxide once in the reservoir can be sufficient over time to penetrate the reservoir seals (both cap rock and lateral seals) (Ennis-King & Paterson, 2005). If CO_2 is able to breach a seal at any point it will ultimately find a pathway out of the reservoir. At high injection rates and pressures, a capillary breakthrough of CO_2 may cause leakage from a reservoir. Interfacial tension (IFT) between CO_2 and reservoir fluids is known to play a vital role in the capillary breakthrough (De Lary, Loschetter, Bouc, Rohmer & Oldenburg, 2012). Therefore, detailed investigations of the IFT behavior between CO_2 and formation fluids are required for each specific subsurface reservoir considered for long-term CO_2 storage to ensure adequate containment can be sustained over time.

Researches focusing on IFT between CO_2 and reservoir fluids have provided in recent years substantial experimental data. Early studies provided IFT measurements for pure water-CO_2 systems in underground conditions dating back to 1957 (Hebach, Oberhof, Dahmen, Kögel, Ederer, & Dinjus, 2002). However, there are concerns about the accuracy of these earlier data measurements due to the questionable assumptions and equations applied (Ennis-King & Paterson, 2005). Yan, Zhao, Chen, & Guo (2001) applied linear-gradient theory to determine IFT for pure water-CO_2 systems at specific temperatures. However, other researchers found out that method tended to underestimate IFT at high pressures and overestimate IFT at low pressures. For salt-water (brine) systems there are much more limited IFT measurements available. Yang & Gu (2004) determined IFT values for a brine-CO_2 system. However, the salinity they studied used was constant and very low, resulting in their observation that salinity did not affect IFT. Previously, Aveyard & Saleem (1975) had reported, however, a linear connection between IFT of brine-CO_2 systems and molal salt concentration under ambient conditions. Two frequently used techniques for measuring IFT of CO_2-brine solutions at high pressures and high temperatures are pendant drop and capillary rise methods (Georgiadis, Maitland, Trusler, & Bismarck, 2010). However, such experimental measurements are time-consuming and require expensive laboratory equipment and sophisticated interpretation procedures.

Mahbob, & Sultan (2016) studied experimentally the changes of interfacial tension and wettability with dolomite rock in the presence of carbon dioxide due to various parameters, such as temperature, pressure, salinity and surfactant type. It was found that with increasing salinity and temperature IFT of brines increases but it decreases with an increase in pressure. These effects are due to the solubility of carbon dioxide in brine. They also concluded that the use of fluoro-surfactants gives the minimum (less than one) interfacial tension. Zhao, Chang, & Feng, (2016) measured the crude oil-carbon dioxide mixture IFT to assess the minimum miscibility pressure. Their research showed that under immiscible conditions, the oil extraction and storage capacity improve dramatically as the injection pressure increases. On the other hand, while the pressure is higher than the MMP, the rise in the injection pressure can only cause a slight increase in oil recovery and storage capacity.

A series of slim tube experiments were planned and presented to measure the impact of cold CO_2 on recovery factor in high-temperature reservoirs (Hamdi, & Awang, 2016). They found that low-temperature CO_2 injection into the high-temperature reservoir can result in a slightly higher recovery factor than isothermal injection. The reason for the increase in recovery was attributed, in particular to the reduction of the interfacial tension between CO_2 and reservoir fluids at the injection point. Golkari, & Riazi (2017) measured experimentally the equilibrium IFT of live and dead crude oil-CO_2 systems. The results of the experiment showed that IFT reduces with different trends as the equilibrium pressure for the live oil/CO_2 and dead oil/CO_2 systems increases. However, it increases with temperature. Karaei, Honarvar, Azdarpour, & Mohammadian (2017) determined the IFT of CO_2/brine at pressures and temperatures up to 7 MPa and 100°C, respectively. Their study confirmed that interfacial tension of CO_2 and brine can be increased by increasing temperature as well as by decreasing pressure.

The CO_2–brine (NaCl + KCl) IFTs were obtained using the method of pendant drop under the condition of 298–373 K temperature, 3–15 MPa pressure (Mutailipu, Liu, Jiang, & Zhang, 2019). They reported that the CO_2–brine IFTs increase with salinity and temperature and decrease with pressure until they reach a plateau. A linear relationship between the increase in IFT and molality was identified for a CO_2–mixed brine system. Furthermore, all samples became less water-wet just as the state of the CO_2 phase changed from subcritical to supercritical.

An empirical equation with an extended uncertainty of 1.6 $mN \cdot m^{-1}$ was developed to describe the interfacial tension between carbon dioxide and aqueous solutions of the mixed salt system (0.864 NaCl + 0.136 KCl) with total salt molalities between (0.98 and 4.95) $mol \cdot kg^{-1}$ as a function of temperature, pressure, and molality by Li, Boek, Maitland, & Trusler (2012). The results showed that the IFT increases linearly with the molality of the salt solution. A summary of the most important empirical correlations derived by several researchers was compiled by Zhang, Feng, Wang, Zhang, & Wang (2016). However, many of those empirical correlations are inaccurate at high salt concentrations (Li, Wang, Li, Liu, Li, & Lv, 2013). In order to estimate the CO_2–brine IFT more accurately, a newly developed CO_2–brine IFT prediction model based on the alternating condition expectation (ACE) algorithm was proposed by Li, Wang, Li, Liu, Li, & Lv (2013). The CO_2–brine IFT correlation developed resulted in an accurate prediction of the impure CO_2–brine IFT with values of AARE = 10.19% and SD = 13.16%. For captured CO_2 to be stored reliably in underground reservoirs, an extensive and efficient CO_2-brine IFT measuring model has yet to be developed that can concurrently consider both impurities in the CO_2 gas injected and a wide range of water salt concentr at ions. Chen & Yang (2018) generalized an IFT correlation between CO_2 and water. The proposed model was a function of mutual solubility and the reduced pressure of CO_2 in a temperature range of 278.2–469.2 K and a pressure range of 0.10–69.10 MPa. Their model generated good prediction accuracy for IFT between CO_2 and brine, provided the salinity is not too high, as the addition of inorganic salt decreases the solubility of CO_2 in the water while increasing the corresponding IFT.

Artificial neural networks (ANN) are widely used (Toghyani, S., Ahmadi, M. H., Kasaeian, A., & Mohammadi, A. H., 2016; Kahani, M., Ahmadi, M. H., Tatar, A., & Sadeghzadeh, M., 2018) for a variety of applications (Maddah, H., Ghazvini, M., & Ahmadi, M. H., 2019; Ramezanizadeh, M., Ahmadi, M. H., Nazari, M. A., Sadeghzadeh, M., & Chen, L., 2019) and continue to be refined and their prediction accuracy improved (Farzaneh-Gord, M., Mohseni-Gharyehsafa, B., Arabkoohsar, A., Ahmadi, M. H., & Sheremet, M. A., 2020). ANN's mathematical algorithms can provide credible prediction models for the complicated and nonlinear system between inputs and outputs by establishing multiple correlations between the input variables in their hidden layers. (Abbasi, Madani, Baghban & Zargar, 2017). This study applies ANN models with various algorithmic constructions to accurately estimate CO_2-brine IFT from a published dataset of experimental measurements for a wide range of CO_2-brine compositions and pressure and temperature conditions. The novelty aspects of the study are related to the application and performance evaluation of six distinct ANN structures and tuning algorithms. The study identifies the RBF model tuned with particle swarm optimization (PSO) and the RBF model tuned with the farmland fertility algorithm (FFA) as the best performing ANN structures for IFT prediction from its influencing variables.

2. Data Analysis

107 published laboratory measurements of interfacial tension (24.78 to 47.87 mN/m) covering a broad range of conditions: temperatures from 27 to 100 °C; pressures from 48 to 258 bar; salinities from 0.085 to 2.75 M, brine densities from 0.97 to 1.105 g/cm^3; and, CO_2 densities from 0.093 to 0.933 g/cm^3 were compiled from analysis of a published source (Chalbaud, Robin, Lombard, Martin, Egermann & Bertin, 2009). Table 1 lists the value ranges for these variables displayed by the 107 data records. This dataset is divided randomly into 75 data records used for training the ANNs, 16 data records used for testing the ANNs. The remaining 16 data records were used for model validation. The model learns only from training data. The validation data set is used to evaluate a model while tuning, and it indirectly affects a given model. However, the test data set is held independently and is only evaluated once a model is entirely trained.

Table 1. Summary statistics of the variable values of the 107 data points used in this study (Chalbaud, Robin, Lombard, Martin, Egermann & Bertin, 2009)

Parameter	Unit	Min	Max
Temperature	℃	27	100
Pressure	Bar	48	258
Salinity	M	0.085	2.75
Brine density	g/cm^3	0.97	1.105
CO_2 density	g/cm^3	0.093	0.933
IFT (dependent variable)	mN/m	24.78	47.87

Table 2 presents a correlation matrix for the six measured variables in the compiled dataset. It reveals that CO_2-brine IFT has relatively high negative correlations with CO_2 density and pressure but has a very low correlation with brine density. As should be expected, salinity is highly correlated with brine density. CO_2 density has quite a high inverse correlation with temperature and quite a high positive correlation with pressure. There is a direct (positive) relationship between IFT and brine density, salinity and temperature, whereas there is an inverse relationship between IFT and CO_2 density and pressure.

3. ANN Model Architectures

Six distinct neural network algorithms are developed to compare their IFT CO_2-brine predictions with the experimentally measured data records. Three multilayer perceptrons (MLPs), with two hidden layers, and three radial basis functions (RBFs) networks represent the ANN models evaluated. The MLPs were trained by Levenberg-Marquardt (LM), Bayesian regularization (BR) and scaled conjugate gradient (SCG) back-propagation algorithms, respectively. The RBF networks were optimized by particle swarm optimization (PSO), differential evolution (DE), farmland fertility algorithm (FFA) algorithms (Karkevandi-Talkhooncheh, Rostami, Hemmati-Sarapardeh, Ahmadi, Husein, & Dabir, 2018; Rostami, Hemmati-Sarapardeh & Shamshirband, 2018; Shayanfar & Gharehchopogh, 2018), respectively. Figure 1 provides a flow diagram detailing the methodology and structure of the ANN models developed.

In all cases, the mean square error (MSE) was evaluated as the cost function to be minimized. Activation functions applied to the MLPs for the input layer to hidden layer 1, hidden layer 1 to hidden layer 2 and hidden layer 2 to the output layer were tensig, logsig and purelin, respectively. Each hidden later had only seven neurons.

The following control variables were applied to the RBF networks:

For RBF-DE: max neurons (35), spread parameter (1.2111), number of population (30), beta min (0.4), beta max (0.8) and crossover probability (0.2).

Where: beta min = lower bound of scaling factor and beta max = upper bound of scaling factor.

For RBF-FFA: max neurons (35), spread parameter (1.1429), number of population (49), α (0.6), β (0.4), W (1) and Q (0.5).

Where: α, β, and Q are numbers between zero and one. W represents the farmland fertility control variable. The values of these variables used for initiating the algorithm are validated by sensitivity analysis.

For RBF-PSO: max neurons (35), spread parameter (1.2129), number of particles in population (50), W (1), W_{damp} (0.99), C_1 (2) and C_2 (2).

Where: W is inertia weight, W_{damp} is inertia weight damping ratio, C_1 is the local learning coefficient, and C_2 is the global learning coefficient.

4. Results and Discussion

Four standard statistical measures of prediction accuracy, average percentage error (APRE), average absolute percentage error (AAPRE), root mean square error (RMSE) and coefficient of determination (R^2) are derived to compare the relative prediction accuracy of the six neural network models evaluated (Table 3). These prediction accuracy measures are listed separately for the training, testing, and validation subsets of data records and for the respective ANN solutions are applied to all records in the data set. High prediction accuracies are achieved for IFT of CO_2-brine solutions by the six ANN models.

The AAPRE and RMSE values recorded for the independent testing data records (Table 3) reveal that the RBF neural network achieves higher IFT prediction accuracy than the MLP models. The RBF network optimized by farmland fertility algorithm (RBF-FFA) displays the lowest AAPRE for the testing records (1.04253), whereas the RBF-PSO model displays the lowest RMSE (0.510938 mN/m) for the testing records, and RBF-DE displays the highest R^2 value (0.994912) for the testing records. For the solutions applied to all data records, RBF-FFA has the lowest AAPRE (1.077149), whereas RBF-PSO has the lowest RMSE (0.50456 mN/m) and the highest R^2 value (0.99225).

Table 2. Correlation matrix for dataset variables with CO_2 Density and pressure showing the highest correlations with measured IFT

Correlation Coefficient (R)	Temperature (°C)	Pressure (bar)	Salinity (M)	Brine Density (g/cm3)	CO_2 Density (g/cm3)	Measured IFT (mN/m)
Temperature (oC)	1	0.07348	0.01320	-0.46528	-0.63521	0.33548
Pressure (bar)		1	0.02944	0.08701	0.62069	-0.69092
Salinity (M)			1	0.85155	0.04057	0.28946
Brine Density (g/cm3)				1	0.39134	0.02063
CO_2 Density (g/cm3)					1	-0.81331
Measured IFT (mN/m)						1

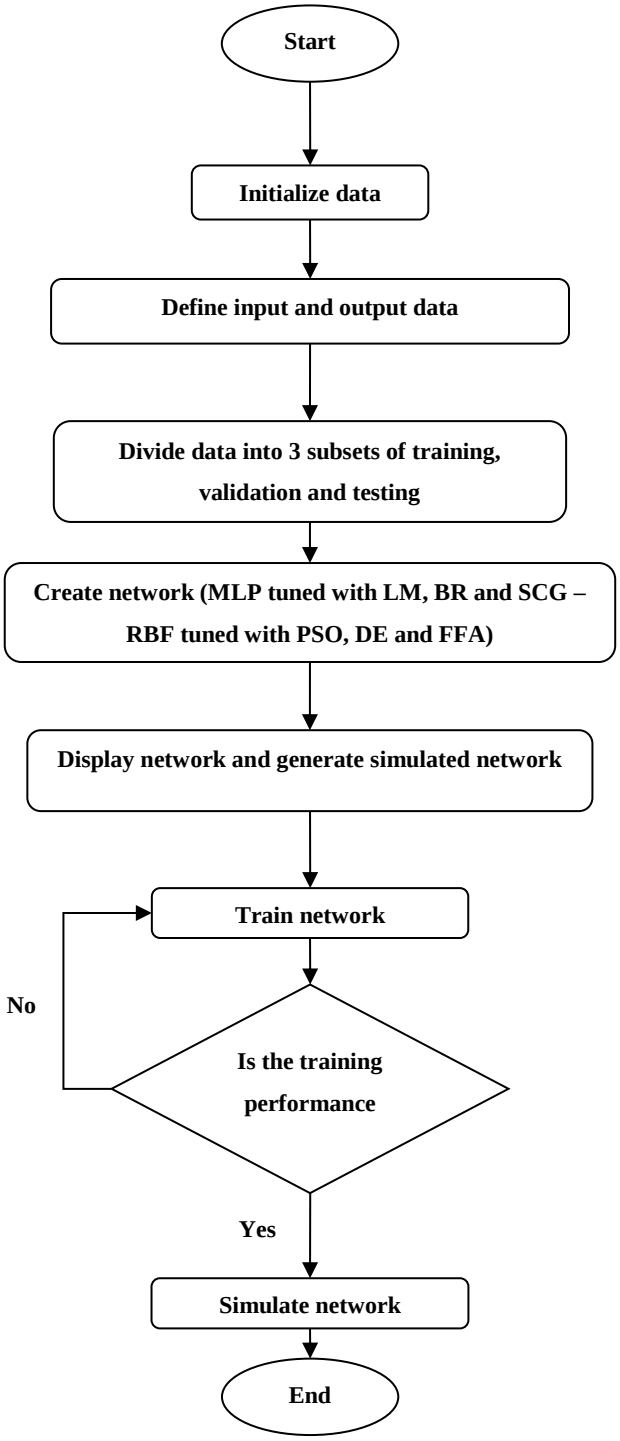

Figure 1. Flow diagram illustrating the ANN methodology adopted.

Table 3. IFT prediction performance of six developed ANN models to predict IFT displaying values for four statistical error metrics. The RBF models show slightly better IFT prediction accuracy than the MLP models.

Model	Type of data	APRE	AAPRE	RMSE mN/m	R^2
MLP-LM	train	0.188446	1.234256	0.526605	0.990742
	test	0.797884	1.550892	0.786258	0.98601
	validation	-0.53192	2.526338	1.057383	0.97125
	all	0.171858	1.474812	0.6738	0.98618
MLP-BR	train	-0.03119	1.146119	0.483051	0.993536
	test	0.235585	1.72654	0.679927	0.98275
	validation	-0.04018	1.700278	0.577608	0.982685
	all	-0.03965	1.321031	0.531575	0.991341
MLP-SCG	train	-0.0061	1.153276	0.47894	0.992929
	test	-0.3173	2.031908	0.859102	0.982914
	validation	-0.86186	1.905514	0.831557	0.971388
	all	-0.1806	1.397145	0.612002	0.988599
RBF-DE	train	-0.0106	1.108915	0.500409	0.99095
	test	-0.57032	1.059825	0.516096	0.994912
	validation	0.300157	1.395466	0.597809	0.991429
	all	-0.04783	1.144423	0.518448	0.991818
RBF-PSO	train	-0.02646	0.941106	0.477718	0.993472
	test	-1.17781	1.346887	0.510938	0.98773
	validation	0.203288	1.728208	0.609664	0.98872
	all	-0.16427	1.119481	0.50456	0.99225
RBF-FFA	train	0.091588	1.108393	0.542889	0.990964
	test	-0.23862	1.04253	0.543982	0.992994
	validation	0.410606	0.96531	0.454816	0.991239
	all	0.089914	1.077149	0.530817	0.991423

Considering only the MLP networks, the MLP network optimized by Levenberg-Marquardt (MLP-LM) displays the lowest AAPRE (1.550892) and highest R^2 value (0.98601) for the testing records, whereas the MLP optimized by Bayesian Regularization (MLP-BR) displays the lowest RMSE (0.679927 mN/m) for the testing records. For the solutions applied to all data records, MLP-BR has the lowest AAPRE (1.321031), the lowest RMSE (0.531575 mN/m) and the highest R^2 value (0.991341). This suggests the MLP-BR model provides the highest IFT prediction accuracy of the three MLP models but is consistently outperformed by the three RBF models.

Figure 2 illustrates the prediction accuracies achieved for IFT of CO_2-brine solutions by the six ANN models in terms of the cumulative frequency of the prediction errors of individual data records when arranged in ascending order for all data records. Whereas all six models display high prediction accuracies for IFT of CO_2-brine solutions, the best performing model in terms of absolute relative error is the RBF-FFA model. For that model, Figure 2 identifies that nearly 70% of the data records involve an absolute relative error of less than 1, and only 3% of the total data records exceeds an absolute relative error of 4.

Figure 3 displays measured experimental IFT for CO_2-brine solutions versus predicted IFT values for each of the six neural network models evaluated for all data records. All data points for the models straddle a line with a 45-degree slope and passing through the origin. This demonstrates the high prediction accuracy achieved collectively by the models, particularly the RBF-FFA and RBF-PSO models. Figure 2 reveals that for the MLP models and the RBF-DE models the greatest dispersion about the unit slope line between measured and predicted data points occurs in the IFT range 26 to 31 mN/m. The RBF-FFA and RBF-PSO models fit the data in that range with much less error than the other models.

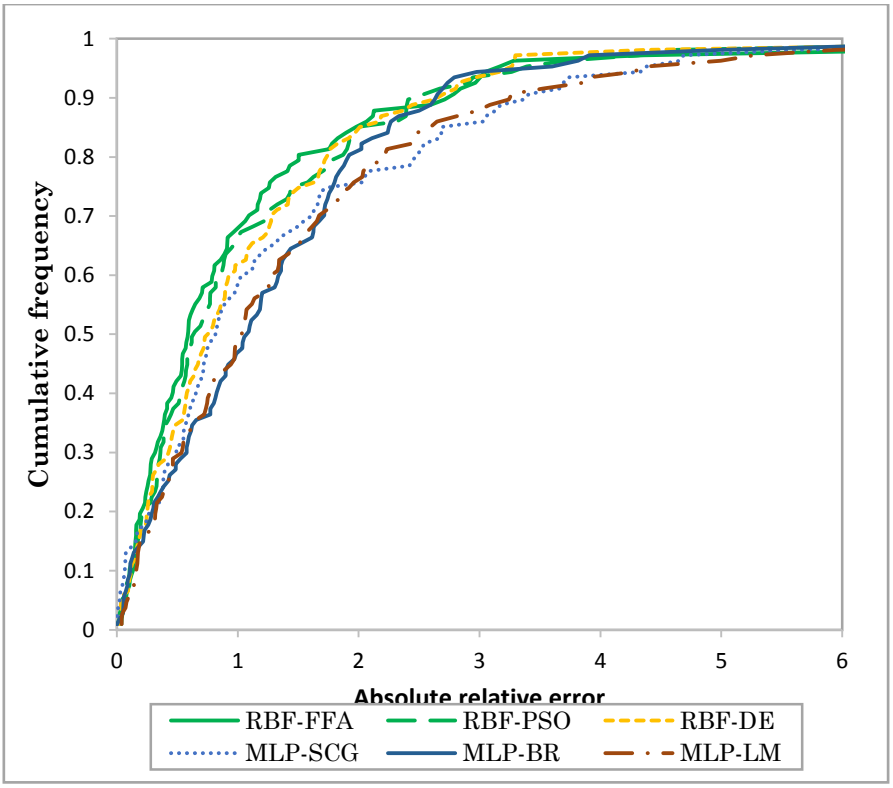

Figure 2. Absolute relative error distribution highlighting that for the RBF-FFA model a higher proportion of the data records have a low absolute relative error compared to the other ANN models

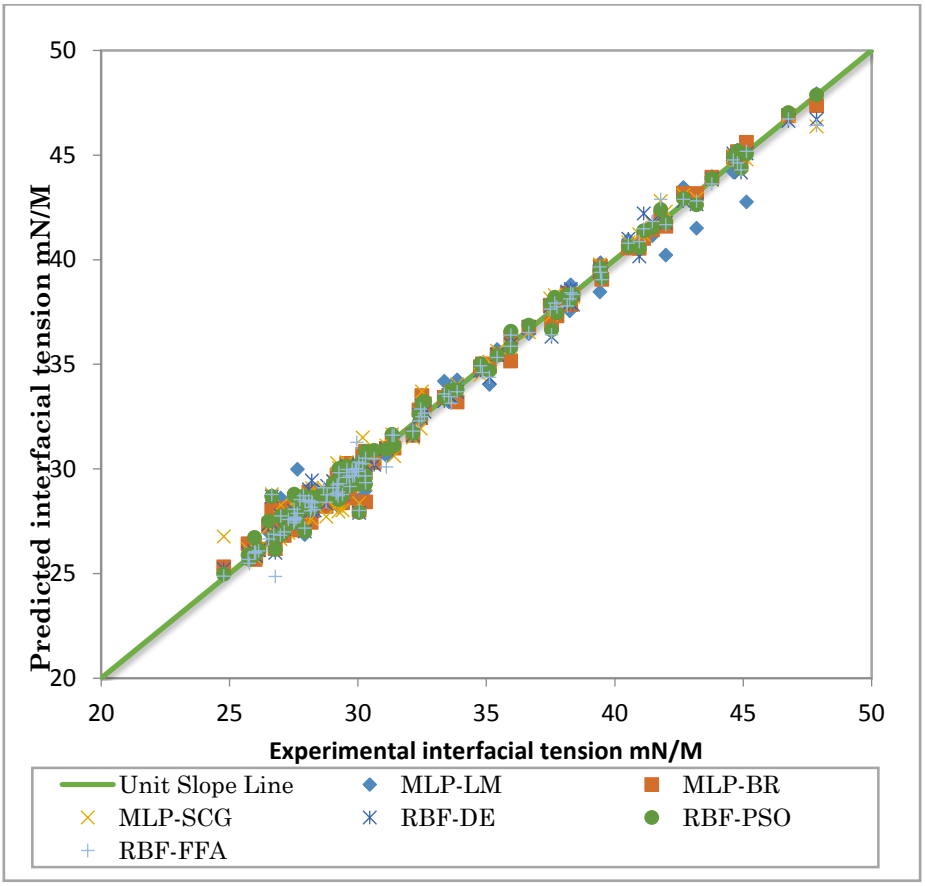

Figure 3. Agreement between predicted and experimental IFT values for the six ANN models. The MLP-LM and MLP-BR models show the greatest scatter. The RBF-PSO and RBF-FFA models show the least scatter

Table 4. Correlation coefficients between predicted IFT for CO_2-brine solutions and the input variables for the six neural network models developed in this study. The models all show similar relationships between their predictions and the input variables confirming their veracity

	Temperature	Pressure	Salinity	Brine density	CO_2 density
MLP-LM	0.3165	-0.6977	0.2879	0.0288	-0.8154
MLP-BR	0.3403	-0.6902	0.2863	0.0154	-0.8171
MLP-SCG	0.338	-0.6956	0.2914	0.0224	-0.8189
RBF-DE	0.3397	-0.6954	0.2876	0.018	-0.8184
RBF-PSO	0.3378	-0.6892	0.2907	0.0218	-0.815
RBF-FFA	0.3363	-0.6903	0.2949	0.0239	-0.8142

Table 4 displays the correlation coefficients (calculated with Excel's CORREL function) between the input variables and the predicted IFT for CO_2-brine solutions. As should be expected, these are all in good agreement with the correlation coefficients displayed in the right-hand column of Table 2 (i.e. between input variable values and the experimentally measure IFT values). Clearly, CO_2 density and pressure are the most influential variables in determining IFT values and both measured and predicted IFT values reflect these relationships.

5. Conclusion

Interfacial tension (IFT) between carbon dioxide (CO_2) and formation fluid (brine) in subsurface reservoirs during CO_2 injection for storage can be predicted with high accuracy by artificial neural networks (ANNs) of various structures. A compilation of laboratory experimental IFT measurements (107 data records) was used to compare the prediction accuracies of IFT for CO_2-brine solutions using six distinct neural network algorithms. Three of the ANN models developed were multi-layer perceptron (MLP) using different training algorithms. The other three ANN models developed were radial basis function (RBF) networks using different training algorithms. 75 data records were used to train the ANNs and 16 data records were used to test and validate them. Each subset was selected randomly without replacement. Analysis of the IFT prediction results indicates that two of the RBF networks outperform the other four ANN models developed and evaluated. The RBF models optimized with the particle swarm optimization (PSO) and farmland fertility (FFA) algorithms both achieved the best prediction performance for IFT of the CO_2-brine solutions. Both of those RBF models generated a prediction performance quantified by RMSE <0.54 mN/m and R^2> 0.99 taking all 107 data records into account.

References

Abbasi, P., Madani, M., Baghban, A., & Zargar, G. (2017). Evolving ANFIS model to estimate density of bitumen-tetradecane mixtures. *Petroleum Science and Technology* 35(2), 120-126.

Abedini, A., & Torabi, F. (2014). On the CO_2 storage potential of cyclic CO_2injection process for enhanced oil recovery. *Fuel* 124, 14-27.

Aveyard, R., & Saleem, S. M. (1975). Interfacial tension at alkane–aqueous electrolyte interfaces. *J C S Faraday* 73, 1613–1617.

Chalbaud, C., Robin, M., Lombard, J. M., Martin, F., Egermann, P., & Bertin, H. (2009). Interfacial tension measurements and wettability evaluation for geological CO_2 storage. *Advances in Water Resources* 32(1), 98-109.

Chen, Z., & Yang, D. (2018). Prediction of equilibrium interfacial tension between CO_2 and water based on mutual solubility. *Industrial & Engineering Chemistry Research* 57(26), 8740-8749.

Damen, K., Faaij, A., & Turkenburg, W. (2003). Health, safety and environmental risks of underground CO_2 sequestration. Copernicus Institute for Sustainable Development and Innovation, Países Bajos.

De Lary, L., A. Loschetter,O. Bouc, J. Rohmer, & Oldenburg, C. M. (2012). Assessing health impacts of CO_2 leakage from a geological storage site into buildings: role of attenuation in the unsaturated zone and building foundation. *International Journal of Greenhouse Gas Control* 9, 322–333.

Ennis-King, J. P, & Paterson, L. (2005). Role of convective mixing in the long-term storage of carbon dioxide in deep saline formations. *SPE Journal* 10(03), 349-356.

Farzaneh-Gord, M., Mohseni-Gharyehsafa, B., Arabkoohsar, A., Ahmadi, M. H., & Sheremet, M. A. (2020). Precise prediction of biogas thermodynamic properties by using ANN algorithm. *Renewable Energy* 147, 179-191.

Georgiadis, A., Maitland, G., Trusler, J. M., & Bismarck, A. (2010). Interfacial tension measurements of the (H_2O + CO_2) system at elevated pressures and temperatures. *Journal of Chemical & Engineering Data* 55(10), 4168-4175.

Golkari, A., & Riazi, M. (2017). Experimental investigation of miscibility conditions of dead and live asphaltenic crude oil–CO2 systems. *Journal of Petroleum Exploration and Production Technology* 7(2), 597-609.

Hamdi, Z., & Awang, M. (2016). Effect of low temperature CO_2 injection in high temperature oil reservoirs using slimtube experiment. *Jurnal Teknologi* 78(6-6), 35-39. https://doi.org/10.11113/jt.v78.9018

Hebach, A., Oberhof, A., Dahmen, N., Kögel, A., Ederer, H., & Dinjus, E. (2002). Interfacial tension at elevated pressures measurements and correlations in the water+ carbon dioxide system. *Journal of Chemical & Engineering Data* 47(6), 1540-1546.

Kahani, M., Ahmadi, M. H., Tatar, A., & Sadeghzadeh, M. (2018). Development of multilayer perceptron artificial neural network (MLP-ANN) and least square support vector machine (LSSVM) models to predict Nusselt number and pressure drop of TiO2/water nanofluid flows through non-straight pathways. *Numerical Heat Transfer, Part A: Applications* 74(4), 1190-1206.

Karaei, M. A., Honarvar, B., Azdarpour, A., & Mohammadian, E. (2017). CO_2 storage in low permeable carbonate reservoirs: permeability and interfacial tension (IFT) changes during CO_2 injection in an Iranian carbonate reservoir. *Periodica Polytechnica Chemical Engineering*. (Published online: 10 October 2019) DOI: 10.3311/PPch.14498

Karkevandi-Talkhooncheh, A., Rostami, A., Hemmati-Sarapardeh, A., Ahmadi, M., Husein, M. M., & Dabir, B. (2018). Modeling minimum miscibility pressure during pure and impure CO_2 flooding using hybrid of radial basis function neural network and evolutionary techniques. *Fuel* 220, 270-282.

Li, X., Boek, E., Maitland, G. C., & Trusler, J. M. (2012). Interfacial tension of (brines+ CO_2):(0.864 NaCl+ 0.136 KCl) at temperatures between (298 and 448) K, pressures between (2 and 50) MPa, and total molalities of (1 to 5) mol· kg–1. *Journal of Chemical & Engineering Data* 57(4), 1078-1088.

Li, Z., Wang, S., Li, S., Liu, W., Li, B., & Lv, Q. C. (2013). Accurate determination of the CO_2–brine interfacial tension using graphical alternating conditional expectation. *Energy & Fuels* 28(1), 624-635.

Maddah, H., Ghazvini, M., & Ahmadi, M. H. (2019). Predicting the efficiency of CuO/water nanofluid in heat pipe heat exchanger using neural network. *International Communications in Heat and Mass Transfer* 104, 33-40.

Mahboob, A., & Sultan, A. S. (2016). An experimental study of interfacial tension and contact angles of CO_2/brines/surfactants/oil systems with dolomite rock. In SPE Kingdom of Saudi Arabia Annual Technical Symposium and Exhibition 25-28 April, Dammam, Saudi Arabia.. Society of Petroleum Engineers. SPE-182839-MS. 5 pages.

https://doi.org/10.2118/182839-MS

McGrail, B. P., Schaef, H. T., Ho, A. M., Chien, Y. J., Dooley, J. J., & Davidson, C. L. (2006). Potential for carbon dioxide sequestration in flood basalts. *Journal of Geophysical Research,* 111, B12201, 13 pages. doi:10.1029/2005JB004169

Mutailipu, M., Liu, Y., Jiang, L., & Zhang, Y. (2019). Measurement and estimation of CO_2–brine interfacial tension and rock wettability under CO_2 sub-and super-critical conditions. *Journal of Colloid and Interface Science* 534, 605-617.

Metz, B., Davidson, O., De Coninck, H., Loos, M., & Meyer, L. (2005). IPCC special report on carbon dioxide capture and storage. Intergovernmental Panel on Climate Change, Geneva (Switzerland). Working Group III.

https://www.ipcc.ch/report/carbon-dioxide-capture-and-storage/ [accessed 27 Jan 2020]

Pranesh, V. (2018). Subsurface CO_2 storage estimation in Bakken tight oil and Eagle Ford shale gas condensate reservoirs by retention mechanism. *Fuel* 215, 580-591.

Ramezanizadeh, M., Ahmadi, M. H., Nazari, M. A., Sadeghzadeh, M., & Chen, L. (2019). A review on the utilized machine learning approaches for modeling the dynamic viscosity of nanofluids. *Renewable and Sustainable Energy Reviews*, 114, 109345.

Rostami, A., Hemmati-Sarapardeh, A., & Shamshirband, S. (2018). Rigorous prognostication of natural gas viscosity: Smart modeling and comparative study. *Fuel* 222, 766-778.

Shayanfar, H., & Gharehchopogh, F. S. (2018). Farmland fertility: A new metaheuristic algorithm for solving continuous optimization problems. *Applied Soft Computing* 71, 728-746.

Toghyani, S., Ahmadi, M. H., Kasaeian, A., & Mohammadi, A. H. (2016). Artificial neural network, ANN-PSO and ANN-ICA for modelling the Stirling engine. *International Journal of Ambient Energy* 37(5), 456-468.

Wood, D. A., & Choubineh, A. (2018). Transparent machine learning algorithm offers useful prediction method for natural gas density. *Gas Processing Journal*. 6 (2), 1-14. DOI: 10.22108/gpj.2018.112015.1035

Yan, W., Zhao, G. Y., Chen, G. J., & Guo, T. M. (2001). Interfacial tension of (methane+ nitrogen) + water and (carbon dioxide+ nitrogen) + water systems. *Journal of Chemical & Engineering Data* 46(6), 1544-1548.

Yang, D., & Gu, Y. (2004). Interfacial interactions of crude oil-brine-CO_2 systems under reservoir conditions. In SPE Annual Technical Conference and Exhibition 26-29 September, Houston, Texas, USA. Society of Petroleum Engineers. SPE-90198-MS, 12 pages. https://doi.org/10.2118/90198-MS

Zhang, J., Feng, Q., Wang, S., Zhang, X., & Wang, S. (2016). Estimation of CO_2–brine interfacial tension using an artificial neural network. *The Journal of Supercritical Fluids* 107, 31-37.

Zhao, H., Chang, Y., & Feng, S. (2016). Oil recovery and CO_2 storage in CO_2 flooding. Petroleum Science and Technology 34(13), 1151-1156.